Lawrence Berkeley National Laboratory
LBL Publications

Title
Experimental validation for thermal transmittances of window shading systems with perimeter gaps

Permalink
https://escholarship.org/uc/item/3pb2q8rr

Journal
Journal of Building Performance Simulation, 11(6)

ISSN
1940-1493

Authors
Hart, Robert
Goudey, Howdy
Curcija, D Charlie

Publication Date
2018-11-02

DOI
10.1080/19401493.2018.1436192

Peer reviewed

eScholarship.org Powered by the California Digital Library
University of California

Lawrence Berkeley National Laboratory

Experimental Validation for Thermal Transmittances of Window Shading Systems with Perimeter Gaps

Robert Hart

Howdy Goudey

D. Charlie Curcija

Lawrence Berkeley National Laboratory

Energy Technologies Area
2018

DOI:
https://doi.org/10.1080/19401493.2018.1436192

Disclaimer:

This document was prepared as an account of work sponsored by the United States Government. While this document is believed to contain correct information, neither the United States Government nor any agency thereof, nor the Regents of the University of California, nor any of their employees, makes any warranty, express or implied, or assumes any legal responsibility for the accuracy, completeness, or usefulness of any information, apparatus, product, or process disclosed, or represents that its use would not infringe privately owned rights. Reference herein to any specific commercial product, process, or service by its trade name, trademark, manufacturer, or otherwise, does not necessarily constitute or imply its endorsement, recommendation, or favoring by the United States Government or any agency thereof, or the Regents of the University of California. The views and opinions of authors expressed herein do not necessarily state or reflect those of the United States Government or any agency thereof or the Regents of the University of California.

Experimental Validation for Thermal Transmittances of Window Shading Systems with Perimeter Gaps

Virtually all residential and commercial windows in the U.S. have some form of window attachment, but few have been designed for energy savings. ISO 15099 presents a simulation framework to determine thermal performance of window attachments, but the model has not been validated for these products. This paper outlines a review and validation of the ISO 15099 centre-of-glass heat transfer correlations for perimeter gaps (top, bottom, and side) in naturally ventilated cavities through measurement and simulation. The thermal transmittance impact due to dimensional variations of these gaps is measured experimentally, simulated using computational fluid dynamics, and simulated utilizing simplified correlations from ISO 15099. Results show that the ISO 15099 correlations produce a mean error between measured and simulated heat flux of 2.5 +/- 7 percent. These tolerances are similar to those obtained from sealed cavity comparisons and are deemed acceptable within the ISO 15099 framework.

Keywords: building energy; windows; window attachments; shading; U-factor; heat transfer

Introduction

Virtually all windows within homes and commercial buildings in the U.S. has some form of shade, blind, drape or other window attachment, but few have been designed for energy savings. High performance solutions for residential and commercial window attachments therefore offer large short-term energy savings potential. Due to the wide variety of window attachment solutions, energy savings can be accomplished in all climates by utilizing systems that reduce heating energy, reduce cooling energy, or both. These products can also reduce mechanical heating and/or cooling system sizing and improve indoor thermal comfort. Some high-performance products are available today but more rapid market adoption would be facilitated by better optimization and selection criteria, e.g. fair performance comparison and rating labels. There are also opportunities to re-engineer and enhance existing products to dramatically improve their performance, both in terms of intrinsic properties and in operations.

In order to provide a common basis of comparison, and to design more cost effective high performance window attachments, it is important to have validated simulation tools. These tools enable rapid design development and optimization through the use of parametric analysis and solution optimization. Several different approaches to simulate windows with attachments have been studied and developed. The primary focus of these works has been the experimental measurement, simulation, and simplified model development of solar heat gain for horizontal (venetian) blinds located between-glass and room-side. An extensive literature review of these studies is provided by Hart et al. (2017) in a companion paper to this work.

Relatively little research has been done to characterize the night-time (zero solar load) U-factor impacts of attachment products other than horizontal blinds, including in-plane products such as solar screens, roller shades, cellular shades, insect screens, and drapes. Existing experimental work includes guarded heater plate measurements of room side and between glass solar screens made by Grasso et al. (1990), Grasso and Buchanan (1979), Fang (2001), Wang et al. (2015), Kotey et al. (2009) and Cuevas et al. (2010), and insect screens by Brunger et al. (1999). Simulation and simplified model development of these products is even less extensive but Fang, Wang, and Kotey do include simplified model development along with their experimental work. Ventilated glazing, or air-flow windows, can be representative of in-plane shading systems. Experiments and model development has been done for these windows, but primarily with forced, rather than natural ventilation, by Carlos and Corvacho (2014), Carlos et al. (2011), Tanimoto and Kimura (1997), and Ismail and Henríquez (2005).

The thermal performance of in-plane products can, in general, be simulated similar to sealed (insulating) glazing with modifications to account for long-wave (IR) radiant transmission, gas flow across attachment layers, and shape factors affecting convection over the surface. The most general solution approach for sealed cavities is to determine convection in asymmetrically heated vertical channels, as shown by Aung (1972) and Roeleveld (2009). To account for unsealed cavities, Wright (2008) developed a resistance network model and van Dijk and Oversloot (2003) developed a model utilizing buoyancy driven pressure difference modifications to the surface convection coefficient of sealed cavities to account for gas flow across layers. The van Dijk model is utilized in ISO 15099 (2003) and the WIS (van Dijk et al. 2003) and Lawrence Berkeley National Laboratory (LBNL) developed Berkeley Lab WINDOW simulation programs (Carli 2006). Collins and Wright (1998) showed that early implementations of this model incorrectly accounted for IR transmission through layers, but this has since been corrected in the Berkeley Lab WINDOW software. Laouadi (2009) expands on the van Dijk/ISO 15099 model by adding product type specific correlations for equivalent properties, flow between layers, and surface coefficients. When applied to ventilated window systems, the ISO 15099 model divides the openings into four distinct openings; top, bottom, sides (equal left and right), and surface (front). While these equations are physically based, the standard does not cite any validation of the approach through either measurements or detailed numerical simulation.

LBNL has developed specialized thermal models based on the ISO 15099 framework for several attachment types including: cellular shades, vertical louvered blinds and perforated screens. In addition, the Complex Glazing Database (CGDB), a database containing complex product optical performance data, has been completed and publicly released. In order to have confidence in the newly developed attachment models, they must be validated through extensive testing and detailed CFD simulation. This paper outlines a review and validation of the ISO 15099 centre-of-glass (COG) heat transfer correlations for naturally ventilated cavities through measurement and simulation. The focus is on the impacts of room-side perimeter ventilated cavities (top, bottom, and side gaps), such as those found with interior in-plane window attachments. The impact of system thermal transmittance due to dimensional variations of these gaps is analysed.

Solution Methods

Three basic methods are used in this work to determine heat flux though window plus attachment configurations; physical testing, detailed two-dimensional CFD simulations with fluid flow solved explicitly, and simplified one-dimensional correlations. Physical testing by means of steady state measurements is performed for model validation, but the method has greater uncertainty and noise between individual measurements than simulations. Two-dimensional finite element conjugate heat transfer and computational fluid dynamics (FEM) simulation incurs the fewest simplifying assumptions and therefore has potential to be the most accurate simulation method, but the method has significant set-up time and slow convergence making the cost impractical for certification standards. ISO 15099 correlation based simulations represent the three-dimensional heat flux through windows in one-dimension. These correlations are implemented in the Berkeley Lab WINDOW software developed by LBNL and are the quickest solution method, at the expense of several simplifying correlations.

Correlations

General sealed cavities

Aspect ratio (AR) is the ratio of height to width of the cavity between glazing and shade. Heat flux through constant-wall-temperature high-AR rectangular fluid-filled cavities has been extensively studied by others such as El Sherbiny et al. (1982), Wright (1996), and Zhao et al. (1998). The work by El Sherbiny et al. is the basis for the sealed cavity model in the ISO 15099 standard. All of these studies provide a means to calculate average heat flux based on simulated or empirical functions involving the non-dimensional Nusselt and Rayleigh numbers as shown in equations 1-3.

$$Nu = f(Ra) \tag{1}$$

$$Nu = \frac{q \cdot L}{k \cdot \Delta T} \tag{2}$$

$$Ra = \frac{\rho^2 \cdot g \cdot C_p \cdot \beta \cdot \Delta T \cdot L^3}{k \cdot \mu} \tag{3}$$

where:

Nu:	Nusselt number	[-]
Ra:	Rayleigh number	[-]
q:	Heat flux	[W m^{-2}]
L:	Characteristic length	[m]
k:	Thermal conductivity	[W m^{-1} K^{-1}]
T:	Temperature	[K]
ρ:	Density	[kg m^{-3}]
g:	Gravity	[m s^{-2}]
C_p:	Heat capacity	[J kg^{-1} K^{-1}]
β:	Coefficient of thermal expansion	[K^{-1}]
μ:	Dynamic viscosity	[Pa s]

The maximum Rayleigh number, based on characteristic length of cavity width, predicted for non-vented enclosed air cavities in the testing scenarios of this work is about 1×10^5. For AR of approximately 30 (as is the case in the test configurations) at such Rayleigh numbers (Ra) multi-cell/secondary laminar flow is predicted. Figure 1, reproduced from Chenoweth (1986), shows that only laminar flow regimes are encountered for the given parameters of this work, and therefore, turbulent flow is not considered here. Because this flow has been widely studied, it provides an excellent basis for the numerical analysis prior to simulating ventilated flow. Non-dimensional analysis of constant wall temperature cavities was performed for AR of 1 to 110 and Ra from 1 to 2.0×10^4 and compared to several previous studies for benchmarking.

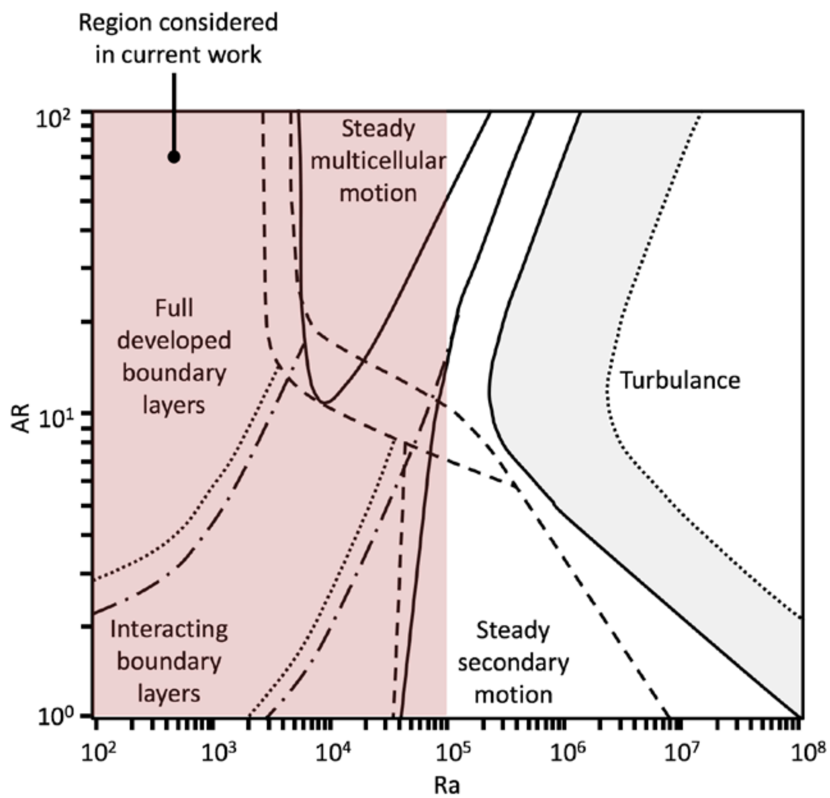

Figure 1. Flow regimes of rectangular cavities with isothermal walls based on height-to-width aspect ratio (AR). The regions encountered in this study are highlighted. The figure is reproduced from Chenoweth (1986).

Window systems and vented cavities

The correlations used in Berkeley Lab WINDOW were developed through a variety of means including laboratory measurements, detailed simulations, and analytical models. The correlations and their sources are defined in ISO 15099. Of specific interest for this work is the model presented for thermally driven ventilation. The model is based on introducing a modifier to the unvented correlation to determine a modified average surface-to-air heat transfer coefficient for the between glass space, $h_{cv,gap}$. The result is solved for iteratively until a prescribed convergence tolerance in gap temperature, T_{gap}, is reached, as presented in Figure 2. The modifying equations are based on several pressure drop principles for air through a channel including Bernouilli, Hagen-Poiseuille, and entrance/exit correlations. While these equations are physically based, the standard does not cite any validation of the approach through either measurements or detailed simulation.

Figure 2. Berkeley Lab WINDOW iterative procedure for thermally driven ventilation heat transfer of room-side shade as described in ISO 15099.

where:

$T_{b,i}$:	back surface temperature of current layer	[K]
$T_{f,i+1}$:	front surface temperature next layer	[K]
T_{room}:	room air temperature	[K]
T_o:	reference temperature, 283 in current work	[K]
T_{av}:	average temperature	[K]
T_{gap}:	equivalent (mean) temperature of air in the cavity	[K]
Z:	pressure loss factor	[-]
μ:	dynamic viscosity of air at mean air temperature	[Pa s]
γ:	tilt angle of space from vertical	[deg]
b:	cavity width	[m]
H:	cavity height	[m]
H_o:	characteristic height (temperature penetration length)	[m]
$h_{c,gap}$:	surface-to-surface heat transfer coefficient by conduction/convection for non-vented cavities	[W m^{-2} K^{-1}]
$h_{cv,gap}$:	surface-to-air heat transfer coefficient by conduction/convection for vented cavities	[W m^{-2} K^{-1}]
P_{tot}:	driving pressure between cavity and room	[Pa]
V:	mean velocity of air flow in cavity	[m s^{-1}]
A_{in}:	equivalent inlet opening area of cavity	[m^2]
A_{out}:	equivalent outlet opening area of cavity	[m^2]
A_s:	cross section area of cavity	[m^2]
A_l:	area of the left side opening	[m^2]
A_r:	area of the right side opening	[m^2]
A_t:	area of the top opening	[m^2]
A_b:	area of the bottom opening	[m^2]
A_f:	area of the holes in surface	[m^2]

Steady state measurements

Industry standard quantitative measurement of window heat flux is performed with calorimetric "hot box" instruments as outlined in ISO 12567 (ISO 2010). An alternative method utilizing calibration transfer standards (CTS) (ASTM 2014) is used for the current work. Figure 3 illustrates the test chamber configuration. The chamber is typically configured to closely match NFRC 100 (2010) boundary conditions of T_c = -18 °C, h_c = 26 W m^{-2} K^{-1} and T_w = 21 °C, h_w determined by natural convection. Where T_c and T_w are the temperatures on the cold and warm sides of the test chamber and h_c and h_w are the surface-to-air heat transfer coefficients.

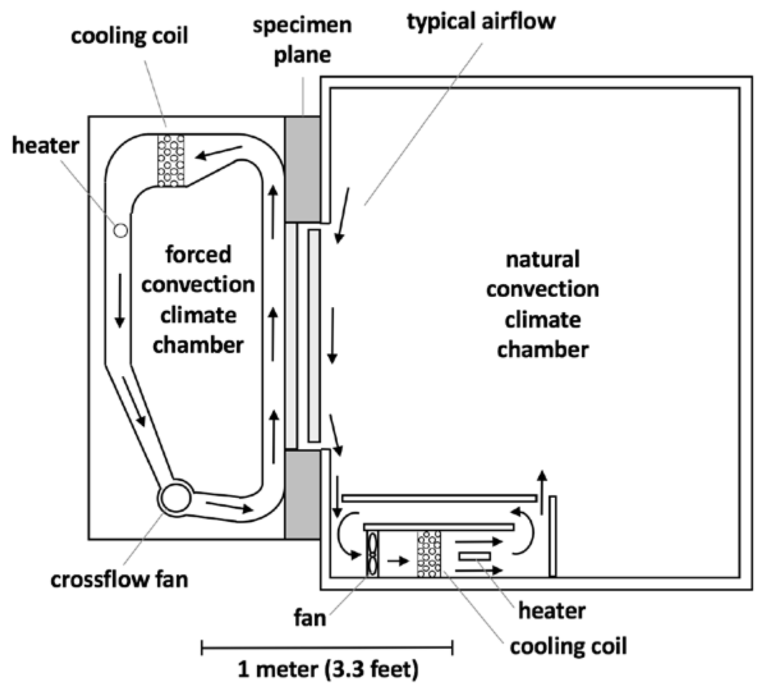

Figure 3. Schematic cross-section of environmental test chambers used for steady state heat flux measurements

Experiments were performed using specially instrumented specimens representing the typical thermal resistances of a glazing system and a shade layer. Both the glazing layer and the shading layer are constructed like CTS, samples of known thermal resistance with many temperature pair measurements that allow for calculation of local heat flux through the specimen in many locations. Thermocouples are placed in an equally spaced 3 x 6 grid (18 per surface) on the inside surface of two 1080 mm by 775 mm glass panes with a calibrated foam layer between. Figure 4 illustrates the configuration of the CTS specimens utilized for this study and the locations of the sensing thermocouples, T_{CTS}. The measured temperatures are taken to represent the average temperature of the immediate area, A, surrounding each sensor.

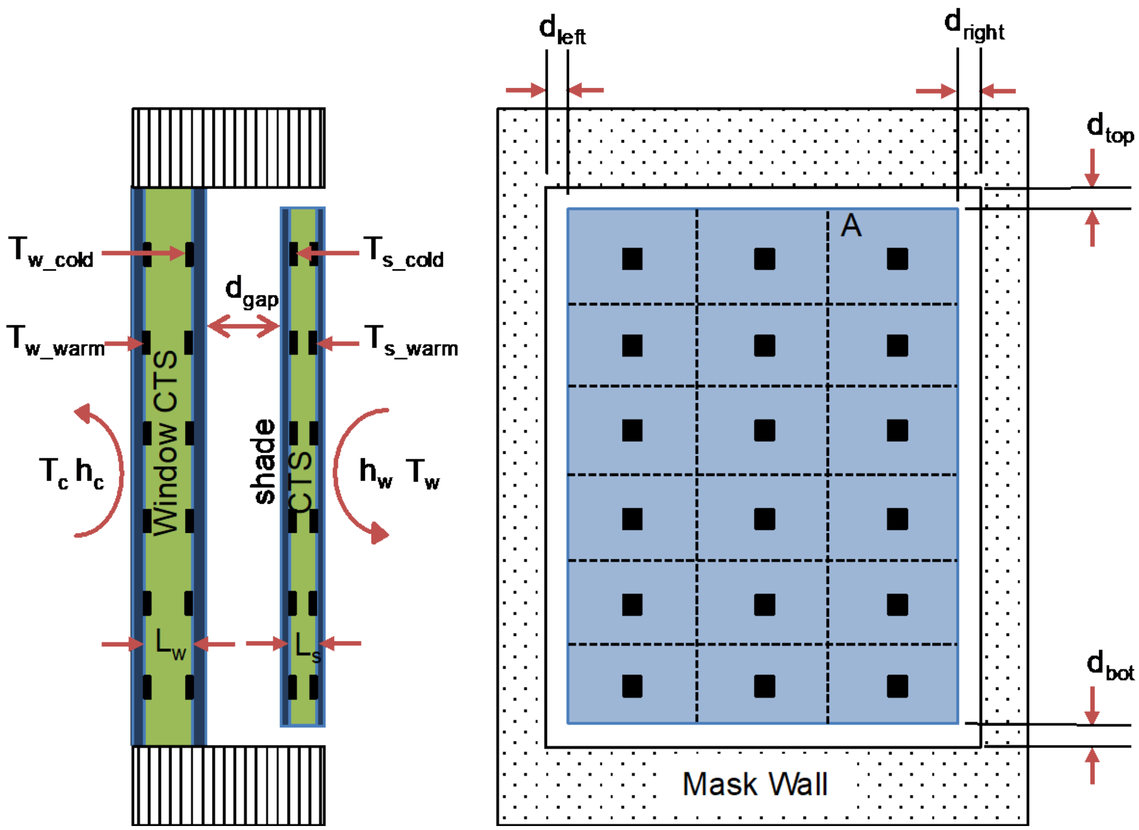

Figure 4. Side and front views of the two-layer CTS assembly placed in the specimen mounting plane mask of the environmental chambers.

Heat flow through window and attachment systems must be determined in both sealed and ventilated configurations of the attachments. Ventilated heat flow, Q_v, is calculated by determining the difference between the heat flow through the "window" portion of the system, Q_w, and heat flow through the "shade" layer, Q_s (Eq. 4). When the shade system is sealed, Q_v equals zero and the same quantity of heat (with minor losses through sides) flows through the window and shade systems. Heat flow through the window and shade system is determined by equations 4 to 7 with the calculated thermal conductivity, k, thickness, L, and measured temperatures $T_{warm/cold}$, on either side of the layers. All derived performance characteristics (such as heat flow and surface coefficients) are calculated for each grid area, A, and then summed over the entire specimen area to determine the overall performance of the system. Heat flux, q, is then calculated by dividing by the total specimen surface area.

$$Q_v = Q_w - Q_s \quad (4)$$

Where:

$$Q = \frac{k_w}{L_w} \sum A \left(T_{w\_warm} - T_{w\_cold}\right) \tag{5}$$

$$Q_s = \frac{k_s}{L_s} \sum A \left(T_{s\_warm} - T_{s\_cold}\right) \tag{6}$$

$$q = \frac{Q}{A_{total}} \tag{7}$$

Computational Fluid Dynamics (CFD) model by the Finite Element Method (FEM)

The multiphysics finite element program COMSOL is used to solve the coupled heat and fluid-flow equations in two dimensions. Conduction, convection, and radiation are simulated explicitly. COMSOL default meshing was used to construct the computational domains. Viscous dissipation is not addressed and all thermophysical properties are assumed to be constant except for the buoyancy term of the y-momentum equation where the Boussinesq approximation is used. The parallel direct iterative sparse solver (PARDISO) was used. Radiation heat transfer was included in the simulations through use of the surface to surface (S2S) direct area integration radiation model, which calculates the energy exchange between surfaces taking into account their size, separation distance and orientation. The S2S model ignores absorption, emission and scattering phenomena of the gas. COMSOL default meshing was used to construct the computational domains. A uniform rectangular mesh was constructed with minimum criteria of two elements within the boundary layer thickness, δ, based on equation 8 for laminar flow. Sensitivity analysis of the solved heat flux was performed at the minimum and maximum Ra extremes to ensure that results are independent of mesh density to less than 1 percent.

$$\delta = L\left(Ra\frac{L}{H}\right)^{-0.25} \qquad [8]$$

For ventilated cases involving only top and/or bottom gaps, two-dimensional finite element analysis can be used because top and bottom gaps are assumed to run the entire width of the surface and all thermophysical properties are assumed to be constant except for the buoyancy term of the y-momentum equation. 2-D analysis greatly reduces computational effort compared to three-dimensions so the detailed numerical investigation is limited to top and bottom gaps for this initial phase of work. Additionally, computational effort is limited by ensuring the height of the specimen and width between glass and shade is chosen to restrict air to the laminar flow regime.

Typical 2D geometry and prescribed boundary conditions for the CFD simulations are shown in Figure 5. Heat transfer through general sealed cavities was solved for using the non-dimensional parameters shown in Figure 5a. Simulations to match as-tested conditions were constructed to match the dimensions and conditions of the test chamber as accurately as possible with the parameters shown in Figure 5b.

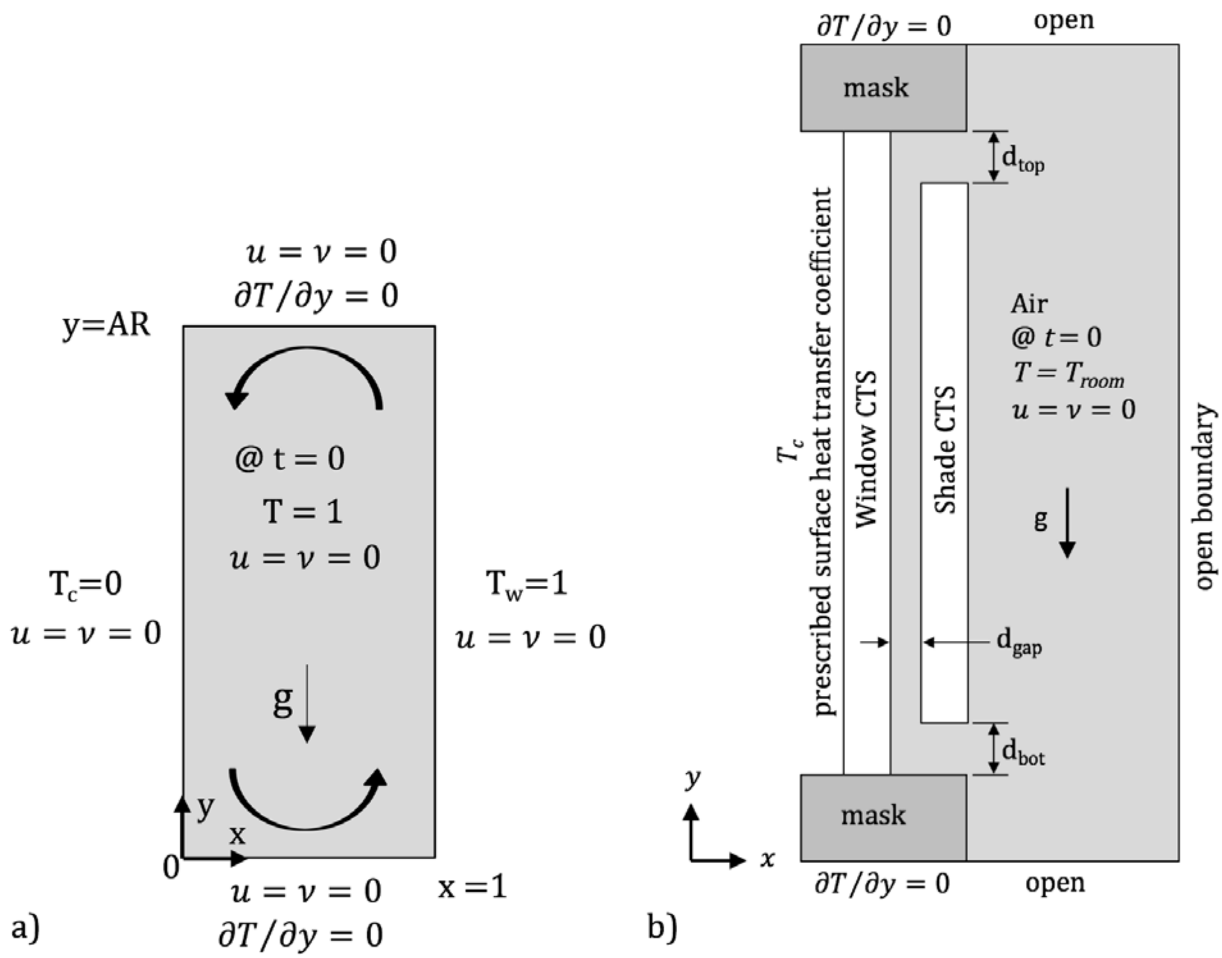

Figure 5. Typical geometry and boundary conditions for a) baseline general sealed cavity CFD simulations, and b) CFD simulations to match measurement parameters

Experimental Design

Six parameters are investigated in depth for perimeter gap scenarios; inside to outside temperature differential, shade to window gap depth, and left, right, top, and bottom gap-width dimensions. The ranges of these parameters are listed in Table 1. A total of 67 different combinations of the six parameters are measured and simulated using the simplified simulation model. The detailed CFD investigation is limited to 19 top and bottom gap configurations as previously described.

Table 1. Measurement parameters for perimeter gap investigation

Variable	Parameter	Set points	Unit
T_c	Cold side Temperature	-18,-10, 0	°C
d_{gap}	Shade-window gap depth	6.4, 12.7, 25.4	mm

d_{left}	Left gap width	0, 4.8, 12.7	mm
d_{right}	Right gap width	0, 4.8, 12.7	mm
d_{top}	Top gap width	0, 2.4, 4.8, 12.7	mm
d_{bot}	Bottom gap width	0, 2.4, 4.8, 12.7	mm

Boundary conditions

The experimental surface-to-air heat transfer coefficient on the warm side is due to natural convection and is therefore relatively small. For unvented shade systems, common flat plate correlations for the natural convective heat-transfer coefficient on vertical surfaces, such as those used by ISO 15099, provide an accurate approximation while reducing computational effort. Vented cavity cases though are more complex and fluid flow must be solved explicitly to determine infiltration. Therefore, a multiphysics approach of solving explicitly for both heat transfer and fluid flow is used for the warm side in all cases. The FEM boundary conditions are assigned to match as closely as possible to the steady-state measurement conditions as follows:

- Warm side: Radiation - surface to ambient temperature (21 °C)

  Convection - solved explicitly
- Cold side: Combined radiation and convection to ambient temperature (-18 °C). Piecewise cubic fit to measured values

Forced convection on the cold side is very complicated to characterize since the as-tested geometry is somewhat complex, the flow is turbulent, and the uniformity of fan flow in the experiment is unpredictable. The most accurate match of simulation to the measured conditions is to therefore assign the measured local combined surface coefficients to the cold side surface directly. Since the CTS used in the experiment has limited measurement points, approximations for the overall surface coefficients are used. Calculated coefficients from the measured temperatures are area weighted, resulting in a step function approximation. The resulting coefficients are then weighted over the entire area into a single value and used in the simplified Berkeley Lab WINDOW model. A piecewise cubic fit between calculated coefficients is used in the FEM model in order to avoid convergence errors due to non-continuous measured step functions. The cold side surface heat transfer coefficient is sufficiently large so that its resistance is small compared to the overall system resistance and, although it cannot be neglected, small deviations in the assigned numerical coefficient from the as-tested conditions have minor impact to the overall system performance. For this reason, the same cold side surface coefficient curve calculated for the unvented cavity measurement is assigned to all as-tested FEM simulations, as shown in Figure 6.

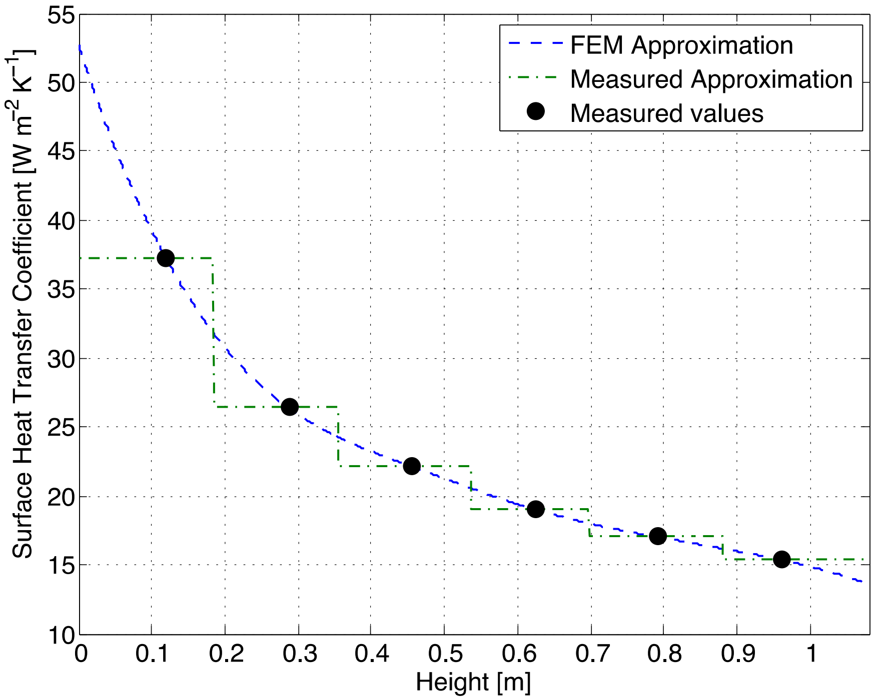

Figure 6. Cold side surface-to-air heat transfer approximation methods based on measured values at 18 locations (6 unique window heights).

Results and analysis

The three methods outlined above are used to compare several representative ventilated gap scenarios to verify the accuracy of the ISO 15099 correlations. General sealed rectangular cavities are first checked against the literature and then compared to as-tested results for sealed cavities in order to gain confidence in the numerical methods. Measured heat transfer through ventilated cavities with perimeter gaps is subsequently compared to simulation to verify the accuracy of the ISO 15099 ventilated cavity heat transfer modification.

General sealed cavities

Figure 7 shows the correlation between the current CFD simulations and previous simulations performed by Zhao et al. (1998) and ISO 15099 (2003) for two different cavity AR. The Zhao model results are fairly typical for CFD simulations, but are only validated up to Ra = 2.0×10^4, which is the typical high end for window systems. With shading systems though, a large gap between the window glass and the shade produces much higher Ra, so Ra = 1.0×10^5, which corresponds to a 25.4 mm gap at the as-tested boundary temperatures is also modelled. The current work predicts cavity heat transfer similarly to industry-accepted Zhao model results, which instils confidence in the more detailed as-tested simulation results. The ISO 15099 model diverges significantly from Zhao and the current work at large Ra. The simplifications in the ISO model from the original work of El Sherbiny, et. al. (1982) produce this divergence.

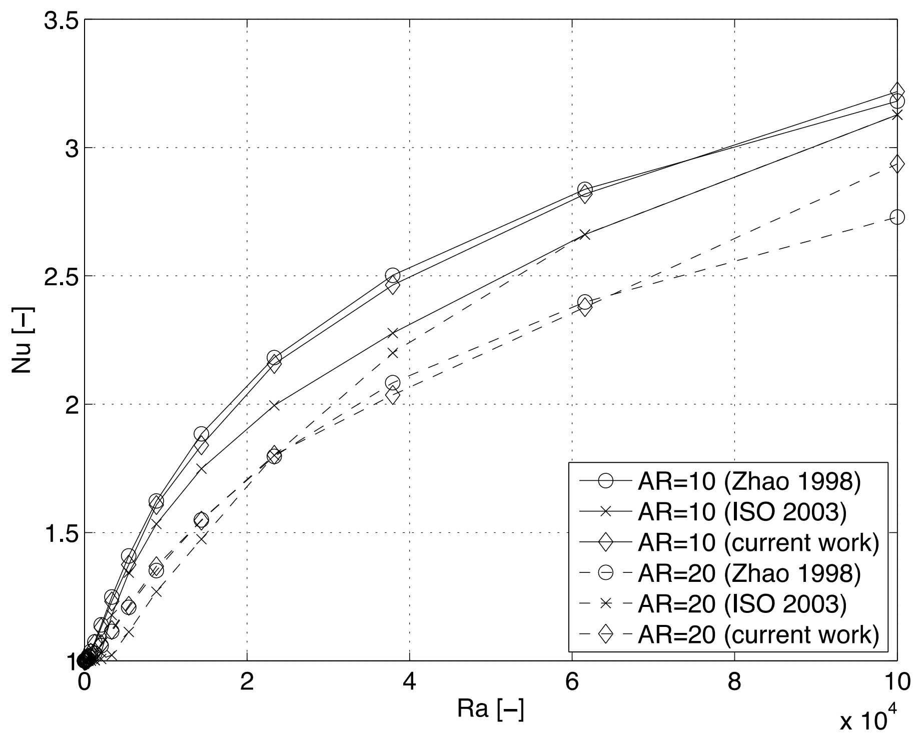

Figure 7. Nu = f(Ra) correlation curves for current work compared to Zhao (1998) and ISO 15099 (2003)

Sealed cavity at physical test conditions

Measured and simulated results for heat flux and surface temperatures from the three evaluation methods (measurement, 1D correlation simulation (Berkeley Lab WINDOW), and 2D FEM simulation) are compared over the height of the test specimen in Figures 8 and 9. Integrated, or averaged, results for each parameter are summarized in Table 2. The average heat flux of the shade CTS is slightly less than the window CTS due to losses through the mask wall cavity perimeter. This edge heat loss is seen in both the FEM and experimentally measured results. The Berkeley Lab WINDOW model assumes adiabatic walls on the cavity perimeter so no difference is seen. The figures and table show that both the Berkeley Lab WINDOW and FEM simulation methods predict overall U-factor to within 1.5% of measurements for the sealed cavity configuration investigated.

Error bars are included in both figures to show the measurement variation over the width of the CTS panels. The maximum variation in heat flux encountered along the width was ± 2.5 percent on the window CTS panel. The variation in measured heat flux and surface temperature along the width of the shade CTS panel was less ± 1 percent in all cases. These results show that system performance is nearly constant along the width and the 2D system assumption used for FEM is justified. The FEM also correlates very closely to measurement for all relevant parameters over the height of the test specimen.

Table 2. Comparison of predicted and simulated U-factors for sealed cavity

Method	Window CTS				Shade CTS				U-factor	U-factor
	T_{w_cold} [°C]	T_{w_warm} [°C]	h_{cold} [W m^{-2} K^{-1}]	q_w [W m^{-2}]	T_{s_cold} [°C]	T_{s_warm} [°C]	h_{warm} [W m^{-2} K^{-1}]	q_s [W m^{-2}]	[W m^{-2} K^{-1}]	[% diff]
Measured	-16.34	-4.24	22.87	39.01	3.51	15.35	6.66	38.17	0.99	-
WINDOW	-16.53	-4.68	22.87	39.30	3.34	15.18	6.66	39.30	1.00	0.76%
FEM	-16.12	-4.65	23.76	39.15	3.62	15.39	7.09	39.06	1.00	1.32%

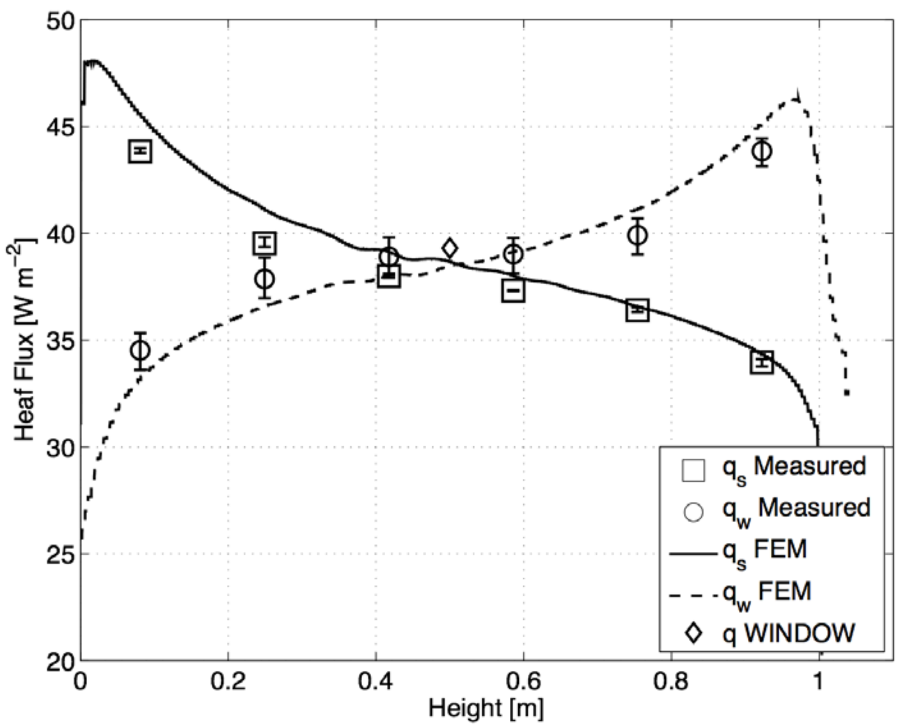

Figure 8. Heat flux through the window CTS as measured and predicted by FEM and Berkeley Lab WINDOW simulations. Error bars on measured results show variation in measurements over the width.

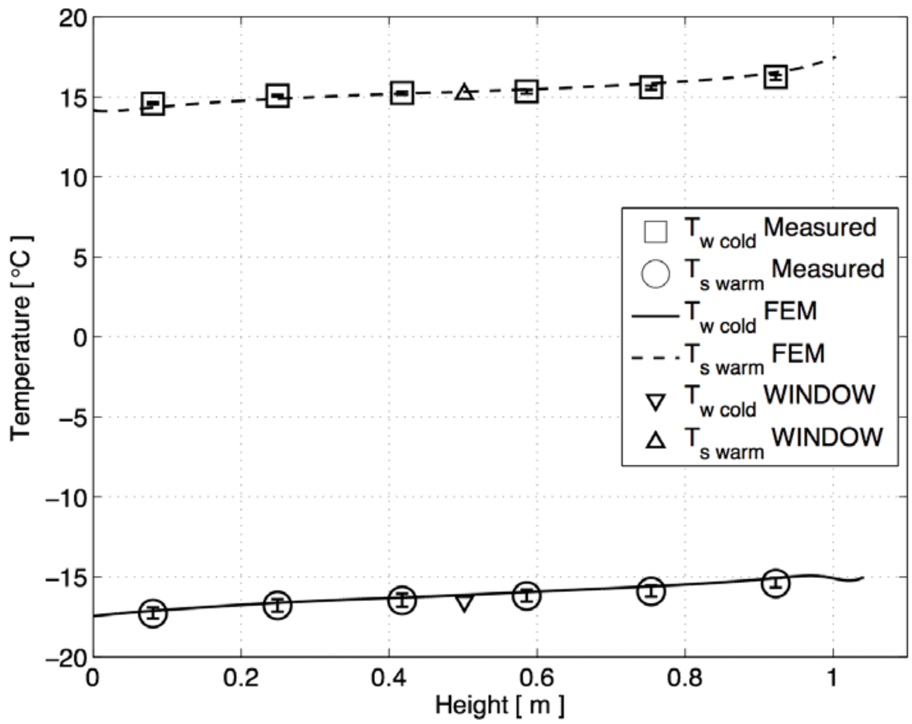

Figure 9. Surface temperatures on exposed surfaces of the test specimen as measured and predicted by FEM and Berkeley Lab WINDOW simulations. Error bars on measured results show variation in measurements over the width.

Ventilated cavity

Simulation

The FEM and Berkeley Lab WINDOW simulated heat flux results for 19 shade configurations with top and bottom gaps are contrasted in Figure 10 with contour plots. Analysis is performed on the basis of heat flux in lieu of thermal transmittance (U-factor) since this property is used in Berkeley Lab WINDOW for simulation convergence. The Berkeley Lab WINDOW/ISO 15099 model assumes flow symmetry, meaning that the same thermal performance is solved for if a pair of ventilation gap dimensions at the top and bottom are swapped. The FEM results support the Berkeley Lab WINDOW model approximation by showing little to no variation in performance by swapping the ventilation gap dimension. The figure also highlights that the minimum gap dimension between top and bottom dominates the ventilation heat flux and is the primary driver of ventilated gap thermal performance. The variation in heat flux between simulation methods is well within ±5% for all cases modelled.

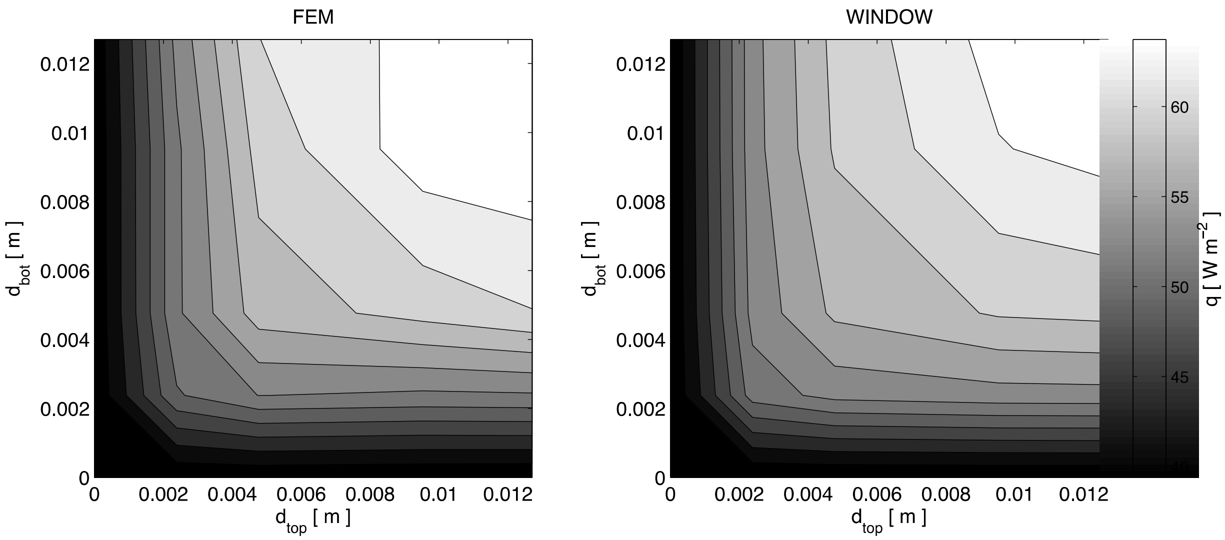

Figure 10. FEM (a) and Berkeley Lab WINDOW (b) heat flux contour maps based on top and bottom ventilation gap dimensions. Results show that performance is symmetric and dominated by the minimum gap dimension.

Measurements

Figure 11a shows the correlation between the Berkeley Lab WINDOW simulation and measured heat flux for all 67 measured perimeter gap combinations. Simulated heat flux is typically less than ±5% from measured results, but the spread is greater than ±10% in some cases. Figure 11b shows several cases where the simulation significantly over predicts heat flux (negative difference), outside of expected probability. A detailed statistical analysis of the data is therefore performed to determine if all measurements are valid and if the WINDOW simulation accurately represents measured performance for all tested configurations.

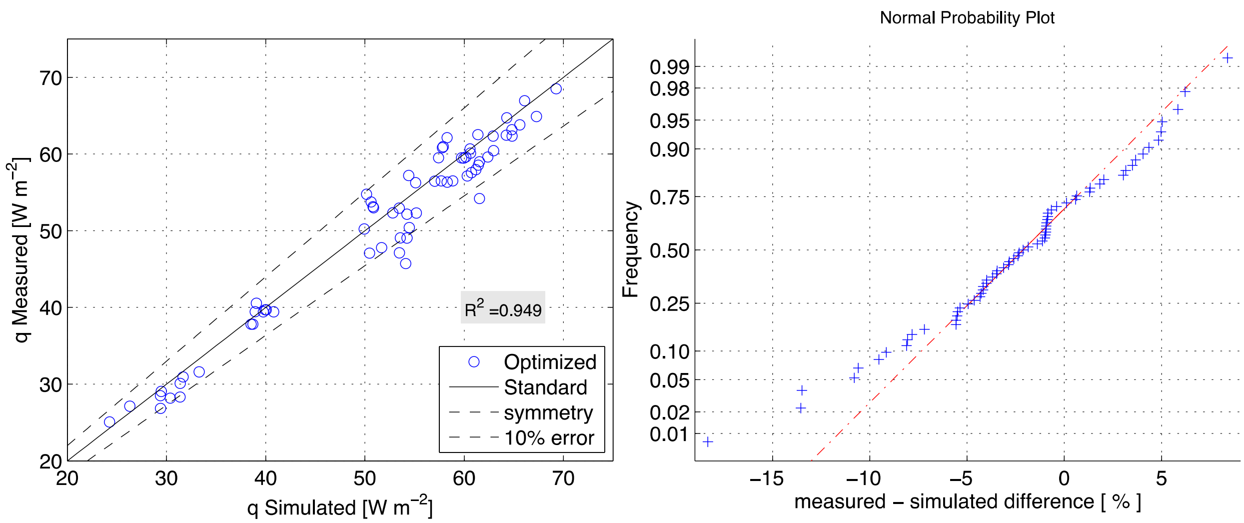

Figure 11. Simulated to measured heat flux comparison for 67 perimeter gap configurations

Minimum gap width

As previously shown in Figure 10, minimum gap width is the driver for ventilated window heat flux. Therefore, an analysis of variance (ANOVA) on the percent difference between the measured and simulated heat flux for the minimum of the top, bottom, or side gap width is performed and presented in Figure 12 with a box plot. The box plot compactly shows key information. The plot identifies the mean through the red centre line, the 25% and 75% quartiles through the top and bottom edges of the box, the 95% confidence interval of the mean through the notched lines going out from the mean, the range of included data through the dashed line "whiskers", and finally it identifies outliers and excludes them from the analysis as shown by the red pluses. A data-point is considered an outlier if it is more than 1.5 times the interquartile range from either quartile.

Figure 12 shows that the mean heat flux difference for all data falls below perfect symmetry at -2%, which is similar to the results for sealed cavities previously presented. This trend holds for perimeter gaps of 4.8mm and 12.7mm, but the heat flux through 2.4 mm gaps appears significantly overestimated in Berkeley Lab WINDOW, with a mean of -8%. A p-value equal to 0.03 of the 2.4mm gap data compared to all measurements confirms the difference is significant using a 95% confidence interval.

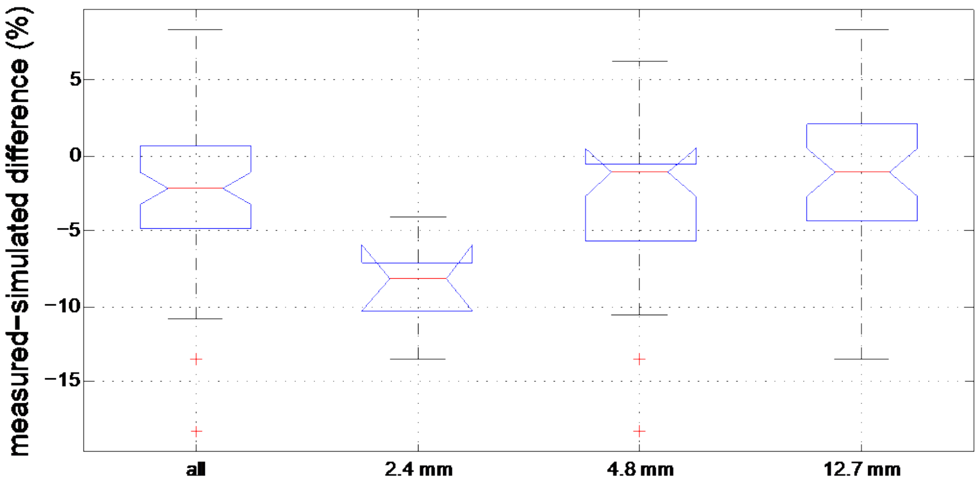

Figure 12. Box plot of percent difference between measured heat flux and Berkley Lab WINDOW simulated heat flux, grouped by all data and the minimum perimeter gap width in each measurement; 2.4 mm, 4.8 mm, and 12.7 mm.

There are several potential drivers for the poor correlation between simulation and measured performance when one or more gaps is 2.4 mm, the smallest gap size considered in this work. The primary driver is likely the difficulty of maintaining such small gaps over the 775 mm width of the tested shade CTS. Each CTS weighed approximately 18 kg, so although the mask-wall foam was quite rigid it did deflect under the CTS load. One measure taken in the experiments to maintain the gaps was adding spacers along the edge of CTS. The addition of spacers though introduced flow restrictions, which are not accounted for in the models. Figure 13 shows a typical IR false-colour image of one such test scenario, where it is clear the introduction of the spacer at mid width and at the edges has restricted the ventilation airflow resulting in warmer temperatures where the surface has not been washed with cooler ventilated air. The figure also shows an additional location where flow is significantly restricted, most likely due to dimensional tolerances in the test system. The effects of these flow restrictions cannot be accurately accounted for so the 2.4 mm data is excluded from the correlation analysis and remains an area for future validation.

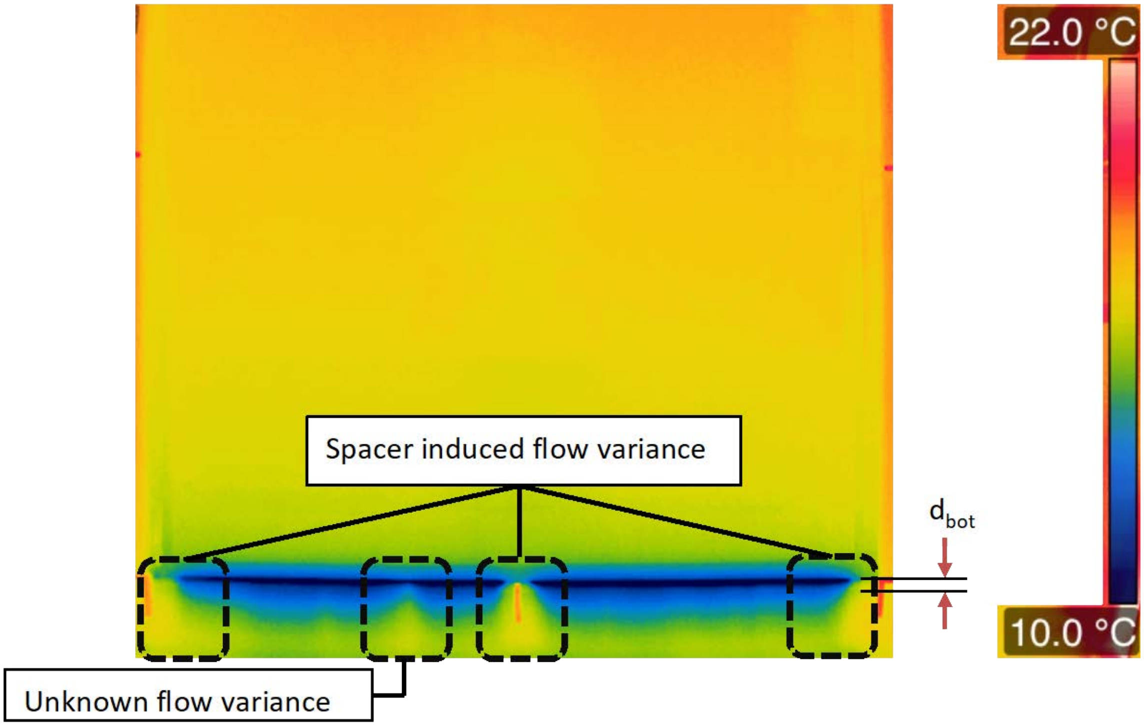

Figure 13. IR thermography false-colour image of ventilated gap area showing surface temperatures impacted by cold airflow from the gap space. Restrictions placed in the air flow path introduce unaccounted for interruptions in gap ventilation air.

Gap location

The previous gap width analysis is based on all combinations of perimeter gaps grouped together. An additional division of the data is performed to isolate all possible gap configurations and ensure there are no biases for certain configurations. The groups are divided in Figure 14 by eight different combinations of top (T), bottom (B), left side (L), and right side (R) gap configurations. The results show that none of the configurations have means significantly different from any other (minimum p-value = 0.43), so the particular perimeter gap configuration is not significant in the difference between Berkeley Lab WINDOW calculation and measured results.

While not statistically significant for this analysis, the L or R and T or B configurations have much larger differences than other configurations from the mean of all data at 7% and 5% respectively. This underestimation of the heat flux by Berkeley Lab WINDOW can likely be attributed to the form of the pressure loss factor (Z) equation from Figure 1. The pressure loss factor equation is dominated by the sealed edges when only one edge is ventilated. The resulting error is relatively small so an examination into the form of the pressure loss factor equation is saved for future research.

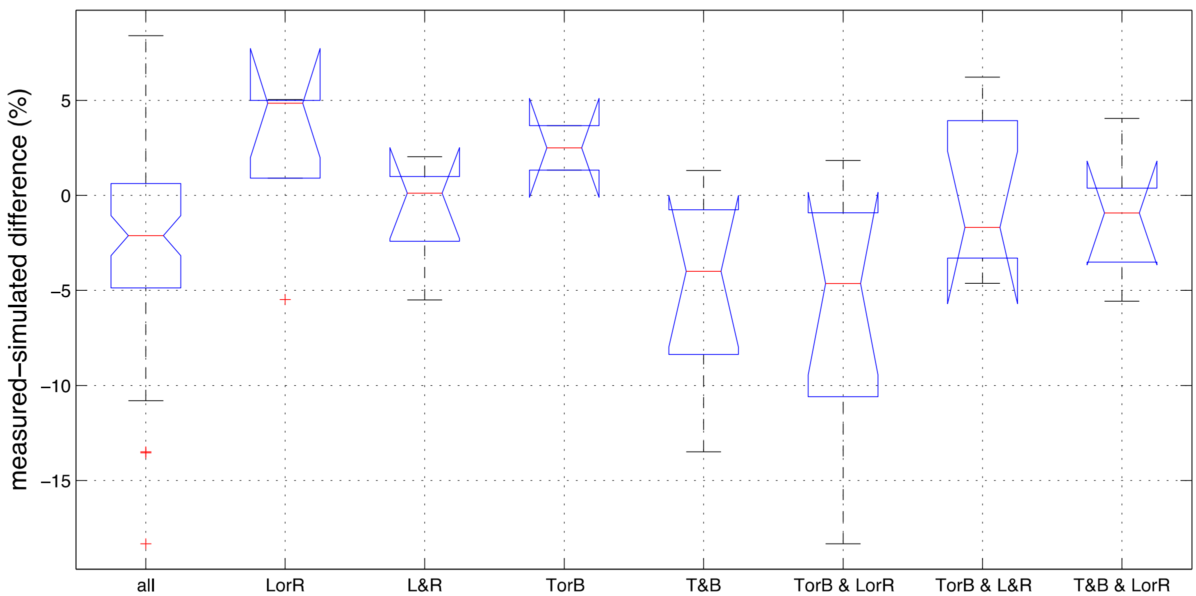

Figure 14. Box plot based on measured to Berkeley Lab WINDOW simulated difference in heat flux grouped by perimeter gap top (T), bottom (B), left side (L), and right side (R) configurations

Three unique data points are identified as outliers in Figure 12, two in 4.8mm group and one in the "all" group. One additional unique outlier is identified in the L or R group of Figure 14. Including the 2.4mm gap group from Figure 12, a total of seven unique measurements are identified. While these measurements may be valid, they are excluded from the correlation analysis, resulting in a total of 60 unique configurations.

All configurations

Perimeter gaps enter into the Berkeley Lab WINDOW/ISO 15099 model as part of the equivalent inlet and outlet opening area calculations. The form of this model lends itself to two correlation constants; C1 for left and right gap widths; and C2 for top and bottom gap widths as shown in Equations 9 and 10. These correlation constants are calculated according to an optimization based on maximizing the coefficient of determination, R^2, between the simulated and measured heat fluxes of the dataset. This is accomplished through the MATLAB constrained nonlinear optimization function, fmincon, with the interior-point algorithm.

$$A^*_{l,r} = \mathrm{C1} \cdot A_{l,r} \quad (9)$$

$$A^*_{t,b} = \mathrm{C2} \cdot A_{t,b} \quad (10)$$

Utilizing the revised algorithm as described and optimizing the correlation coefficients based on measured data, correlation coefficients of C1 = 0.99 and C2 = 0.92 are obtained. The accuracy of the simulation increases insignificantly when utilizing the correlation coefficients as shown in Figure 15. Therefore, correlation coefficients of C1 = 1, and C2 = 1 as are currently implemented in Berkeley Lab WINDOW are recommended.

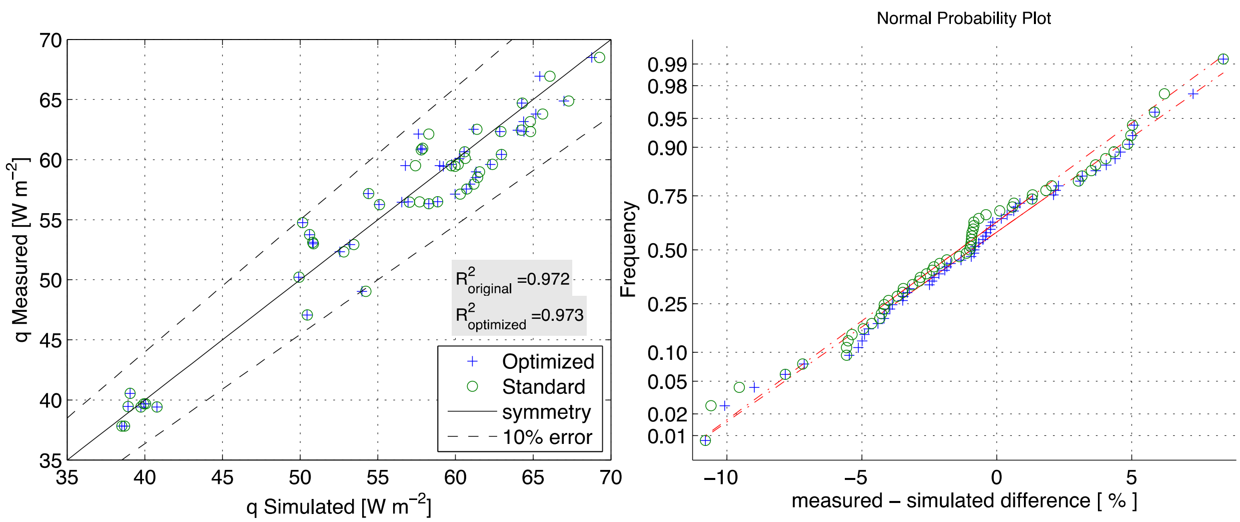

Figure 15. Optimized and standard WINDOW correlations of simulated to measured heat flux comparison for 60 perimeter gap configurations

Comparison to measurements from literature

The limited existing experimental work focusing on perimeter gaps of interior mounted attachments include guarded heater plate measurements made by Grasso (1979), Fang (2001), Wang (2015), Kotey (2009), and Cuevas (2010). Of these, only the model developed by Fang and the five unique shade materials tested at two different environmental conditions by Grasso provide sufficient detail to emulate measurement and/or simulation parameters. Figure 16 shows Berkeley Lab WINDOW simulation results compared to the previous studies. Parameters are based on those defined by Grasso as shade to glass depth, d_{cavity} of 24.5mm; side gap width, d_{left} and d_{right} of 12.7mm; and top gap width, d_{top} of 25.4mm. Bottom gap width, $d_{bot,}$ is not defined but assumed to be 12.7mm. Boundary conditions match Grasso with natural convection on inside and a cold side wind speed of 0.5 [m s^{-1}]. Fang does not define the dimensions of 'tight' or loose' so both are plotted to give a performance range. The three methods show very good agreement for the range of parameters measured. A fourth curve is plotted based on the EN 13125 standard (2001). This standard defines the additional thermal resistance over base glazing provided by shutters and blinds. The EN 13125 standard shows poor correlation to all other methods.

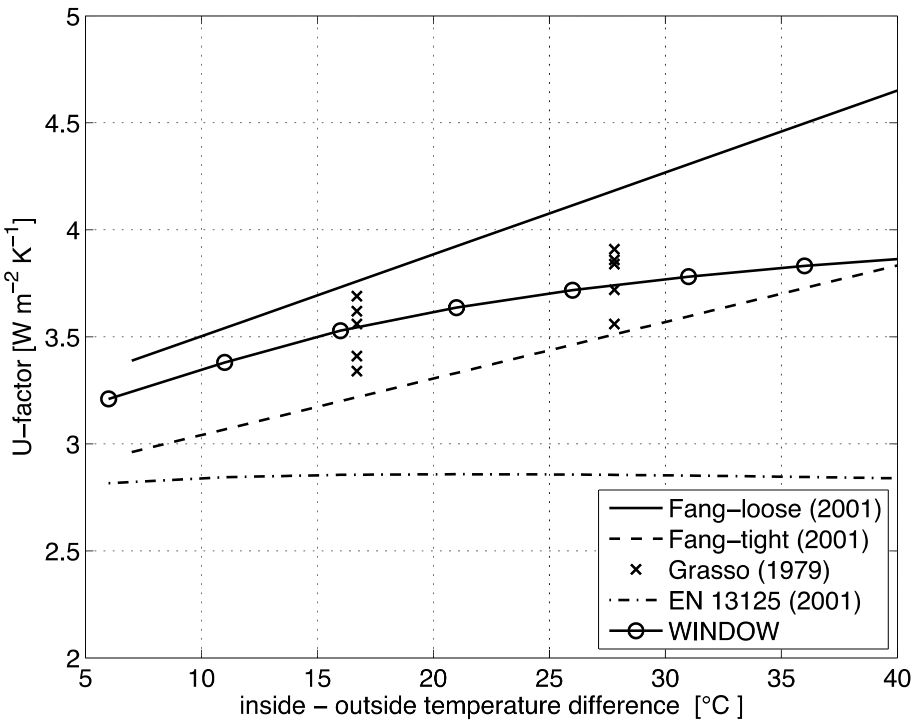

Figure 16. Berkeley Lab WINDOW simulation results for centre-of-glass U-factor of shade over single clear glass as a function of inside-outside temperature difference compared to literature.

Conclusions

The impact on thermal transmittance of window systems with ventilated cavities due to dimensional variations of perimeter (top, bottom, and side) gaps are measured experimentally, simulated using CFD analysis, and simulated utilizing simplified correlations from ISO 15099 as implemented by Berkeley Lab WINDOW. The correlation between 2D FEM and Berkeley Lab WINDOW models for top and bottom gap configurations is within ±5% for all cases examined and shows the simplified Berkeley Lab WINDOW model is a reasonable simulation alternative to detailed CFD analysis for this type of ventilated cavity flow. Further analysis demonstrates that the current Berkeley Lab WINDOW ventilated cavity algorithm accurately represents, within ±10%, real performance for all of the perimeter gap configurations measured. Finally, Berkeley Lab WINDOW simulations are shown to be similar to existing experimental results in the literature. The scope of the presented work is broad in that a majority of all interior mounted window attachment products are installed with some type of unsealed perimeter gap.

Funding

This work was supported by the Assistant Secretary for Energy Efficiency and Renewable Energy, Building Technologies Program, of the U.S. Department of Energy under Contract no. DE-AC02-05CH11231.

References

ASTM International. 2014. *C1199-14 Standard Test Method for Measuring the Steady-State Thermal Transmittance of Fenestration Systems Using Hot Box Methods*. West Conshohocken, Pa.

Aung, W., L.S. Fletcher, and V. Sernas. 1972. "Developing Laminar Free Convection Between Vertical Flat Plates with Asymmetric Heating." *International Journal of Heat and Mass Transfer 15*: 2293-2308.

Brunger, A., F.M. Dubrous, and S. Harrison. 1999. "Measurement of the solar heat gain coefficient and U value of windows with insect screens." *ASHRAE Transactions 105*: 1038-1042.

Carli, Inc. 2006. *Tarcog: Mathematical Models for Calculation of Thermal Performance of Glazing Systems With or Without Shading Devices.* Technical Report. Accessed October 1, 2015. http://windows.lbl.gov/software/window/6/tarcog%20mathematical%20model.pdf

Carlos, J. S., and H Corvacho. 2014. "Evaluation of the thermal performance indices of a ventilated double window through experimental and analytical procedures: Uw-values." *Renewable Energy 63*: 747–754.

Carlos, J. S., H. Corvacho, P.D. Silva, and J.P. Castro-Gomes. 2011. "Modelling and simulation of a ventilated double window." *Applied Thermal Engineering 31*(1): 93–102.

Chenoweth, D.R. and Paolucci, S. 1986. "Natural convection in an enclosed vertical air layer with large horizontal temperature differences". *Journal of Fluid Mechanics* 169: 173-210.

Collins, M., J.L. Wright. 1998. "Calculating Center-Glass Performance Indices of Windows with a Diathermanous Layer." *ASHRAE Transactions 112*: 1–12.

Cuevas, C., A. Fissore, and N. Fonseca. 2010. "Natural convection at an indoor glazing surface with different window blinds." *Energy and Buildings 42*(10): 1685–1691.

van Dijk, D., and H. Oversloot. 2003. "WIS, the European tool to calculate thermal and solar properties of windows and window components." *Proceedings of Building Simulation*: 259–266.

El Sherbiny, S.M., G.D. Raithby, and K. Hollands. 1982. "Heat Transfer by Natural Convection Across Vertical and Inclined Layers." *ASME Journal of Heat Transfer* 104: 96-102.

EN 13125. 2001. *Shutters and Blinds - Additional Thermal Resistance - Allocation of a Class of Air Permeability to a Product*. CEN. Brussels.

Fang, X. 2001. "Study of the U-factor of a window with a cloth curtain." *Applied Thermal Engineering* 21(5): 549–558.

Grasso, M. and D.R. Buchanan. 1979. "Roller Shade System Effectiveness in Space Heating Energy Conservation." *ASHRAE Transactions*, *85*(2520): 156-173.

Grasso, M., B. Hunn, and R. Briones. 1990. "Effect of Textile Characteristics on the Thermal Transmittance of Interior Shading." *ASHRAE Transactions*, *96*(1): 875-883.

Hart, R., H. Goudey, and D.C. Curcija. 2017. "Experimental validation and model development for thermal transmittances of porous window screens and horizontal louvred blind systems" *Journal of Building Performance Simulation*.

International Organization for Standardization 12567-1. 2010. *Thermal performance of windows and doors -- Determination of thermal transmittance by the hot-box method — Part 1: Complete windows and doors.* Geneva.

International Organization for Standardization 15099. 2003. *Thermal Performance of Windows, Doors, and Shading Devices — Detailed Calculations.* Geneva.

Ismail, K. A. R. And J. R. Henríquez. 2005. "Two-dimensional model for the double glass naturally ventilated window." *International Journal of Heat and Mass Transfer 48*(3-4): 461–475.

Kotey, N. A., J. L. Wright, C. S. Barnaby, and M. R. Collins. 2009. "Solar gain through windows with shading devices: Simulation versus measurement." *ASHRAE Transactions 115(2)*: 18–30.

Laouadi, A. 2009. "Thermal performance modeling of complex fenestration systems." *Journal of Building Performance Simulation 2* (3): 189–207.

National Fenestration Rating Council. 2010. *NFRC-100-2010E0A1. Procedure for Determining Fenestration Product U-factors.*

Roeleveld, D., D. Naylor, P. H. Oosthuizen. 2009. "Empirical Correlations for Free Convection in an Isothermal Asymmetrically Heated Vertical Channel." *Heat Transfer Engineering 30(3*): 189-196.

Tanimoto, J. and K. Kimura. 1997. "Simulation Study on an Air Flow Window System with an Integrated Roll Screen." *Energy and Buildings 26*(3): 317–325.

Wang, D., Y. Liu, Y. Wang, Q. Zhang, J, Liu. 2015. "Theoretical and experimental research on the additional thermal resistance of a built-in curtain on a glazed window." *Energy and Buildings 88*: 68–77.

Wright, J.L. 1996. "A Correlation to Quantify Convective Heat Transfer Between Vertical Window Glazings." *ASHRAE Transactions* 102 (1): 940-946.

Wright, J. L. 2008. "Calculating Center-Glass Performance Indices of Glazing Systems with Shading Devices." *ASHRAE Transactions* 114 (2): 199–209.

Zhao, Y., D. Curcija, J. Power, and W. Goss. 1998. "Improved Heat Transfer Correlations for Quantifying Laminar Natural Convection Across Fenestration Glazing Cavities." *Thermal Performance of the Exterior Envelopes of Buildings VII.* Clearwater Beach, FL